

Symmetry of the magneto-optic response of the Sagnac interferometer

J. S. Dodge, L. Klein, M. M. Fejer, and A. Kapitulnik

Department of Applied Physics, Stanford University, Stanford, California 94305

We demonstrate the application of the Sagnac interferometer to magneto-optic measurements at an oblique angle of incidence. With an appropriate choice of polarization states for the two counter-propagating beams, a wide variety of magneto-optic effects may be measured, in the absence of an external perturbing field, with a sensitivity of a few hundred nanoradians. Using simple symmetry analysis of the conventional Kerr rotation measurement geometry, we may distinguish contributions to the non-reciprocal phase shift due to the polar, longitudinal and transverse Kerr effects, and consequently completely determine the magnetization vector direction, averaged over the probed region. Magneto-optic hysteresis loops were taken on a permalloy film to demonstrate the effectiveness of the new technique. We discuss the relevance of the Sagnac interferometer to magnetic microscopy and to the study of magnetic anisotropies in thin films.
© 1996 American Institute of Physics. [S0021-8979(96)47908-3]

The Sagnac interferometer (SI) has proven to be a useful instrument for sensitive magneto-optic (MO) measurements.¹⁻³ Very general arguments based on the Helmholtz reciprocity theorem show that the SI can only be sensitive to effects which break time-reversal symmetry, such as the linear magneto-optic effects.⁴ The selective sensitivity of the Sagnac to MO effects is its chief advantage over conventional, polarimetric measurement techniques, as it allows one to perform measurements with a sensitivity of $500 \text{ nrad}/\sqrt{Hz}$, in the absence of the perturbing magnetic field which is typically used to ensure that the measured effect has a magnetic origin. This advantage is most apparent in applications such as microscopy and magnetic relaxation measurements, which must be performed in constant magnetic field.³ In near-field scanning optical microscopy especially, depolarizing topographic features can be difficult to distinguish from magnetic features, a difficulty which the SI overcomes by its very nature.⁵⁻⁸ In previous work, the application of the SI has been limited to normal-incidence Kerr and Faraday rotation measurements. In this work, we demonstrate the more general application of the SI to magneto-optic Kerr measurements at oblique incidence, and show that symmetry arguments allow us to determine all three vector components of the magnetization by appropriate analysis of the MO response.

The SI measures intensity changes due to interference between counter-propagating waves, from which we can infer the relative phase shift between them.⁹ By using only one of the polarization eigenmodes of a single-mode, polarization maintaining fiber to guide the light through most of its path in the interferometer, we ensure that the two counter-propagating waves travel along identical paths. One wave can then be thought of as the time-reversed reciprocal of the other, and consequently any phase shift between them must result from an effect which breaks time-reversal symmetry. To measure magneto-optic effects in reflection, we break the fiber loop and insert collimating optics, together with the bulk optics shown in Fig. (1). We use pairs of $\lambda/2$ and $\lambda/4$ retardation plates to transform the polarization states from the linear eigenmode of the fiber to arbitrary polarization states, \mathbf{P}_1 and \mathbf{P}_2 , which we write as Jones vectors in a cartesian basis.¹⁰ The polarizers at both ends of the optics train

serve as polarization filters for the reflected beams. The two beams are reflected from a magnetized sample, and the natural coordinate system for describing the magnetization direction, in which we denote each coordinate by the name of its associated magneto-optic effect, is indicated. The only source of non-reciprocal phase shift in the interferometer is the magnetized sample, so we may neglect the rest of the interferometer and calculate only the relative phase shift between the two beams as they traverse the space between two imaginary observation planes \mathcal{O}_1 and \mathcal{O}_2 , indicated in the diagram.

Conceptually, it is helpful to represent the behavior of the single-mode fibers, polarizers and retardation plates by two pairs of idealized optical elements, a polarized planar source and a coherent, polarization sensitive, spatially filtered detector.¹¹ One of each is located at each of the observation planes, as indicated in Fig. 2. We denote each monochromatic source field at its plane of origin \mathcal{O}_i by $\mathbf{E}_i^{\text{src}}(\mathbf{r}, t) = \mathbf{E}_i^{\text{src}}(\mathbf{r})e^{-i\omega t}$, and the field which the source generates at its plane of detection by $\mathbf{E}_i^{\text{src}' }(\mathbf{r}, t) = \mathbf{E}_i^{\text{src}' }(\mathbf{r})e^{-i\omega t}$. The field which the coherent detector at \mathcal{O}_i accepts will simply be the reciprocal of corresponding source field, $\mathbf{E}_i^{\text{det}}(\mathbf{r}, t) = \mathbf{E}_i^{\text{src}*}(\mathbf{r})e^{-i\omega t}$. Throughout, we will assume that both the incident and reflected field amplitudes are described by a single polarization state over the whole field profile, so that we may write $\mathbf{E}_i^{\text{src}' }(\mathbf{r}) = \mathbf{E}_i^{\text{src}' }(\mathbf{r})\mathbf{P}_1$. This assumption will not generally hold if the sample is inhomogeneous, but the treatment given here may be extended to such cases by following the standard treatment in Fourier optics of coherent imaging.^{2,12} In practice, the optics are aligned so that the scalar part of all of the above fields are identical, described approximately by Gaussian functions $E^0(\mathbf{r})$. We may then represent reflection from a material with magnetization vector \mathbf{M} by a reflectivity matrix $R(\mathbf{M})$ which acts only on the polarization state, so that $\mathbf{E}_{1,2}^{\text{src}' }(\mathbf{r}) = E^0(\mathbf{r})R(\mathbf{M})\mathbf{P}_{1,2}$. For fixed source fields, the complex amplitude $\alpha(\mathbf{E}_i^{\text{src}}(\mathbf{r}), \mathbf{E}_j^{\text{src}}(\mathbf{r}), \mathbf{M})$ which the source at \mathcal{O}_i excites in the detector at \mathcal{O}_j will be given by the overlap integral between the two fields:

$$\alpha(\mathbf{E}_i^{\text{src}}(\mathbf{r}), \mathbf{E}_j^{\text{src}}(\mathbf{r}), \mathbf{M}) = \int_{\mathcal{O}_j} \mathbf{E}_j^{\text{det}*}(\mathbf{r}) \cdot \mathbf{E}_i^{\text{src}' }(\mathbf{r}) d\mathbf{r}$$

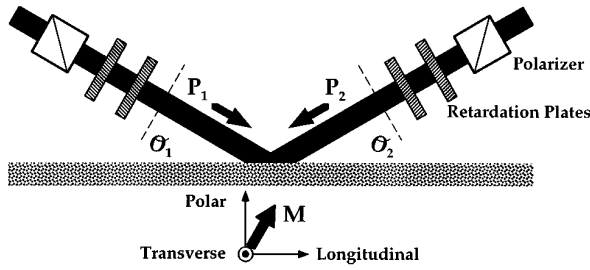


FIG. 1. Bulk optics for measurement at oblique incidence.

$$= \int_{\mathcal{O}_j} \mathbf{E}_j^{\text{src}}(\mathbf{r}) \cdot \mathbf{E}_i^{\text{src}'}(\mathbf{r}) d\mathbf{r},$$

$$\propto \mathbf{P}_j \cdot [R(\mathbf{M})\mathbf{P}_i]. \quad (1)$$

The non-reciprocal phase shift between the beams will be

$$\varphi_{\text{nr}}(\mathbf{E}_i^{\text{src}}(\mathbf{r}), \mathbf{E}_j^{\text{src}}(\mathbf{r}), \mathbf{M}) = \text{Arg} \left(\frac{\alpha(\mathbf{E}_i^{\text{src}}(\mathbf{r}), \mathbf{E}_j^{\text{src}}(\mathbf{r}), \mathbf{M})}{\alpha(\mathbf{E}_j^{\text{src}}(\mathbf{r}), \mathbf{E}_i^{\text{src}}(\mathbf{r}), \mathbf{M})} \right). \quad (2)$$

If the sample is nonmagnetic, then by the symmetry of the kinetic coefficients its dielectric tensor ϵ_{ij} must be symmetric,¹³ and the Helmholtz reciprocity theorem holds:⁴

$$\int_{\mathcal{O}_1} \mathbf{E}_2^{\text{src}'}(\mathbf{r}) \cdot \mathbf{E}_1^{\text{src}}(\mathbf{r}) d\mathbf{r} = \int_{\mathcal{O}_2} \mathbf{E}_1^{\text{src}'}(\mathbf{r}) \cdot \mathbf{E}_2^{\text{src}}(\mathbf{r}) d\mathbf{r}. \quad (3)$$

This implies that the phase shift given by Eq. (2) is zero, as expected. If the sample is magnetized, then the dielectric tensor will develop off-diagonal terms, Eq. (3) no longer holds, and we may detect a non-zero φ_{nr} . The SI is dynamically biased to produce a voltage signal which is proportional to the phase shift multiplied by the average optical power at the detector, so the measured signal is roughly proportional to $\varphi_{\text{nr}} \times |\alpha(\mathbf{E}_i^{\text{src}}(\mathbf{r}), \mathbf{E}_j^{\text{src}}(\mathbf{r}), \mathbf{M})|^2$. The magnitude of the signal due to this non-reciprocity will depend on the details of the optical constants of the material, the nature of the boundary conditions, the polarization states \mathbf{P}_1 and \mathbf{P}_2 , and the direction of the magnetization. Symmetry considerations will help us choose polarization states which provide useful information about the magnetization state under fairly general circumstances, simplifying our analysis considerably.

We consider the case of an isotropic sample magnetized in an arbitrary direction. Shelankov and Pikus have discussed the constraints which time-reversal symmetry, together with a variety of other crystal symmetries, impose on the reflectivity matrix.¹¹ Our analysis parallels theirs, and the reader may refer to their work for more details concerning the in-

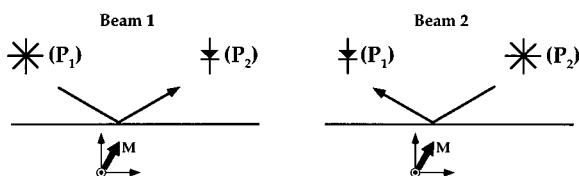


FIG. 2. Idealized schematic of two beams, with planar, monochromatic sources and coherent, polarization sensitive, spatially filtered detectors.

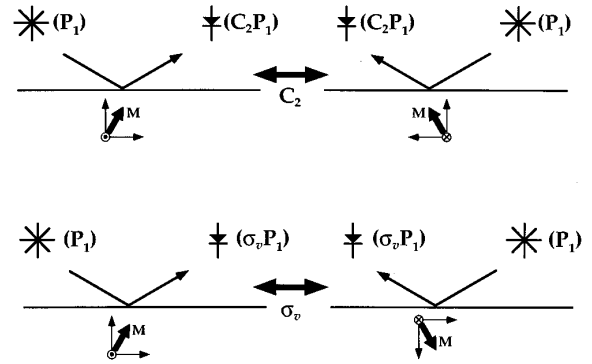


FIG. 3. Symmetries of the experimental apparatus for different choices of the polarization states. When $\mathbf{P}_2 = C_2\mathbf{P}_1$, the polar effect is not measured. When $\mathbf{P}_2 = \sigma_v\mathbf{P}_1$, the longitudinal effect is not measured. The operation σ_v transforms the magnetization as shown because it is a pseudovector. P-polarized states satisfy both symmetries and measure only the transverse effect.

fluence of crystal symmetry and gyrotropy on our results. Neglecting these effects, we can see that there are two transformations which will map the source plane of one beam onto the source plane of the other: (i) C_2 , a 180° rotation about the film normal, and (ii), σ_v , a reflection through the plane perpendicular to both the film surface and the plane of incidence. We may choose \mathbf{P}_1 and \mathbf{P}_2 to satisfy one or both of these symmetries, as shown in Fig. 3. By doing so, we eliminate the contribution of one or more magnetization directions to the magneto-optic response. Consider the case $\mathbf{P}_2 = C_2\mathbf{P}_1$. Rotation changes the sign of both the transverse and the longitudinal components of the magnetization, but leaves the polar component unchanged. Thus symmetry requires that a sample magnetized in the polar direction will have the same response to each beam, producing zero relative phase shift between them, while the magnetization along the transverse or longitudinal directions will typically yield a finite shift. In a similar way, by choosing $\mathbf{P}_1 = \sigma_v\mathbf{P}_2$ we will observe no longitudinal response. If \mathbf{P}_1 and \mathbf{P}_2 are linear, p-polarized states, then both symmetries are satisfied and only the transverse component gives a finite response (s-polarized states, due to their symmetry under reflection in the plane of incidence, yield no response whatsoever). Limiting ourselves to the linear response the magnetization, with coupling constants α , we may summarize these statements by the following equations:

$$\varphi_{\text{nr}}^{\bar{p}}(\mathbf{M}, \mathbf{E}_1^{\text{src}}(\mathbf{r})) \equiv \varphi_{\text{nr}}(\mathbf{E}_1^{\text{src}}(\mathbf{r}), C_2\mathbf{E}_1^{\text{src}}(\mathbf{r}), \mathbf{M})$$

$$= \alpha_{\bar{p},t} M_t + \alpha_{\bar{p},l} M_l, \quad (4a)$$

$$\varphi_{\text{nr}}^{\bar{l}}(\mathbf{M}, \mathbf{E}_1^{\text{src}}(\mathbf{r})) \equiv \varphi_{\text{nr}}(\mathbf{E}_1^{\text{src}}(\mathbf{r}), \sigma_v\mathbf{E}_1^{\text{src}}(\mathbf{r}), \mathbf{M})$$

$$= \alpha_{\bar{l},t} M_t + \alpha_{\bar{l},p} M_p, \quad (4b)$$

$$\varphi_{\text{nr}}^{\bar{p}l}(\mathbf{M}) \equiv \varphi_{\text{nr}}(\mathbf{E}_s(\mathbf{r}), \mathbf{E}_s(\mathbf{r}), \mathbf{M}) = \alpha_{\bar{p}l,t} M_t. \quad (4c)$$

A bar above the magnetization direction indicates that this component is forbidden by symmetry from contributing to the signal. These three phase shifts may all be determined simply by changing the orientations of the retardation plates shown in Fig. 1. By determining the five coupling constants,

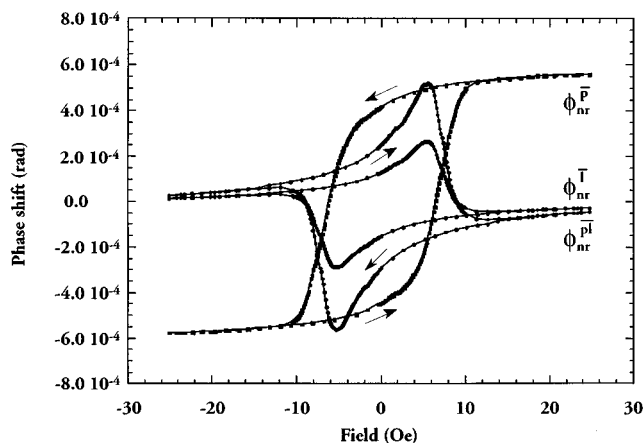


FIG. 4. Raw data from a hysteresis loop in a permalloy film.

we can use Eqs. (4) to calculate the complete magnetization vector from a measurement of the three phase shifts.

To verify this analysis, we have observed hysteresis loops in a permalloy film. Measurements of the three phase shifts described in Eqs. (4) are shown in Fig. 4. In these measurements, the sample was mounted on goniometers for precise alignment to the surrounding optics, and the field was swept with a small horseshoe magnet oriented in the plane of incidence. The field had a small component in the transverse direction, which produced the finite phase shift φ_{nr}^{pl} seen in the saturated part of the loops. All polarizing optics were carefully aligned to satisfy the required symmetry relations; we estimate the error in this alignment to be less than 1 mrad for any one component. In Eqs. (4), the transverse magnetization contributes to all three phase shifts, and must be subtracted. We obtained $\alpha_{\bar{p},t}$, $\alpha_{\bar{l},t}$ and $\alpha_{\bar{p}l,t}$ directly by rotating the magnet to saturate the magnetization in the transverse direction and measuring each of the three phase shifts. We obtained the constant $\alpha_{\bar{p},l}$ in a similar way. We then scaled the hysteresis loop for φ_{nr}^{pl} accordingly and subtracted it from the other two loops. Demagnetization energy forces the magnetization to lie in the plane of the film, and the curves for φ_{nr}^{pl} and $\varphi_{nr}^{\bar{p}}$ are in fact proportional. We could not easily saturate the permalloy in the polar direction to measure $\alpha_{\bar{l},t}$, but after subtracting the transverse contribution to $\varphi_{nr}^{\bar{l}}$, the remaining phase shift was zero within the noise of the measurement, so we may safely take $M_p=0$. Fig. 5 shows the normalized magnetization components M_t and M_l which we derive from the data in Fig. 4. The data nicely show the effectively coherent rotation of the magnetization during much of the loop. As the field is increased from -25 Oe, the magnetization rotates toward the transverse direction. Up to about $+5$ Oe, the magnitude of the magnetization $|\mathbf{M}|$ remains constant as M_t increases. Above 5 Oe, we observe a rounding off of the transverse magnetization, while the longitudinal component switches abruptly. The SI measures the average magnetization in the beam area, so the reduction of $|\mathbf{M}|$ in this field range indicates that the switching occurs by domain formation, preventing φ_{nr}^{pl} from reach-

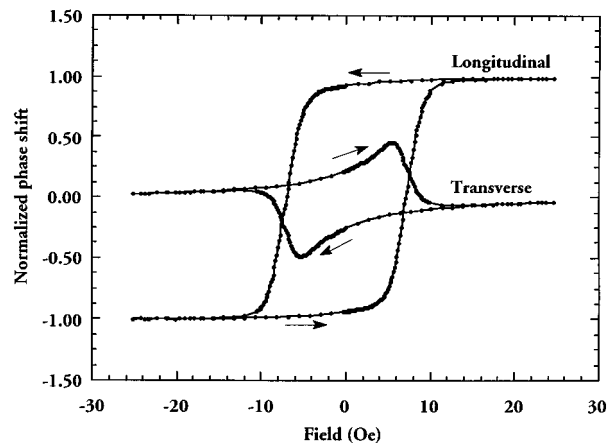


FIG. 5. Normalized magnetization components M_t and M_l calculated from the data in Fig. 4.

ing its maximum value. This behavior is similar to that seen in other thin films with uniaxial anisotropy.¹⁴

We should emphasize that the symmetry properties of the SI allow us to perform these measurements in static or zero applied field as well as for the hysteresis loops shown here. We recently demonstrated the advantage of this capability in normal incidence measurements by correlating the structural domain size in SrRuO₃ with the magnetic domain size observed after cooling through the Curie point in zero field.³ It may be interesting to apply the techniques described here to the study of spin reorientation transitions in epitaxial magnetic films.^{15,16} The ability to discriminate clearly between the longitudinal and the polar orientations is an attribute which could be especially useful here. In microscopy with magneto-optic contrast, these capabilities could be useful for characterizing magnetic anisotropy variations in thin films on a microscopic scale.¹⁷ The symmetry considerations are quite general and can be extended to a wide range of experimental geometries.

¹ S. Spielman, K. Fesler, C. B. Eom, T. H. Geballe, M. M. Fejer, and A. Kapitulnik, Phys. Rev. Lett. **65**, 123 (1990).

² S. Spielman, J. S. Dodge, L. W. Lombardo, C. B. Eom, M. M. Fejer, T. H. Geballe, and A. Kapitulnik, Phys. Rev. Lett. **68**, 3472 (1992).

³ L. Klein, J. S. Dodge, T. H. Geballe, A. Kapitulnik, A. F. Marshall, L. Antognazza, and K. Char, Appl. Phys. Lett. **66**, 2427 (1995).

⁴ L. D. Landau, E. M. Lifshitz, and L. P. Pitaevskii, *Electrodynamics of Continuous Media* (Pergamon, New York, 1984).

⁵ E. Betzig, J. K. Trautman, R. Wolfe, E. M. Gyorgy, P. L. Finn, M. H. Kryder, and C.-H. Chang, Appl. Phys. Lett. **61**, 142 (1992).

⁶ T. J. Silva, S. Schultz, and D. Weller, Appl. Phys. Lett. **65**, 658 (1994).

⁷ B. D. Terris, H. J. Mamin, D. Rugar, W. R. Studenmund, and G. S. Kino, Appl. Phys. Lett. **65**, (1994).

⁸ A. Kapitulnik, J. S. Dodge, and M. M. Fejer, J. Appl. Phys. **75**, 6872 (1994).

⁹ H. Lefevre, *The Fiber Optic Gyroscope* (Artech House, Boston, 1993).

¹⁰ M. A. Azzam and N. M. Bashara, *Ellipsometry and Polarized Light* (North-Holland, New York, 1977)

¹¹ A. L. Shelankov and G. E. Pikus, Phys. Rev. B **46**, 3326 (1992).

¹² S. Spielman, Ph.D. thesis, Stanford University, 1992.

¹³ L. D. Landau and E. M. Lifshitz, *Statistical Physics, Part 1* (Pergamon, New York, 1980).

¹⁴ R. Osgood, R. L. White, B. Clemens (submitted).

¹⁵ Z. Q. Qiu, J. Pearson, and S. D. Bader, Phys. Rev. Lett. **70**, 1006 (1993).

¹⁶ A. Berger, A. W. Pang, and H. Hopster, Phys. Rev. B **52**, 1078 (1995).

¹⁷ R. W. Schafer and A. Hubert, J. Magn. Magn. Mater. **65**, 7 (1987).